LUND UNIVERSITY

Modes of propagation of electromagnetic pulses in closed cylindric bi-isotropic waveguides

Rikte, Sten

2001

[Link to publication](#)

Modes of propagation of electromagnetic pulses in closed cylindric bi-isotropic waveguides

Sten Rikte

Sten Rikte

Department of Electroscience
Electromagnetic Theory
Lund Institute of Technology
P.O. Box 118
SE-221 00 Lund
Sweden

Abstract

Modes of propagation of electromagnetic pulses in closed, cylindric waveguides with bi-isotropic fillings are analyzed systematically using complex, time-varying electromagnetic fields. The emphasis is on the circular bi-isotropic waveguide and the bi-isotropic parallel-plate waveguide. For both geometries, seven Volterra integral equations of the second kind, which are to be solved simultaneously for each specific mode, are derived.

1   Introduction

Time-harmonic wave propagation in chirowaveguides attracted considerable attention during the 1990's. The basic theory of the closed, cylindric chirowaveguide, which consists of a single, hollow, perfect conductor with chiral filling, was presented by Pelet and Engheta [15]. The important case with circular cross section was analyzed in detail in [6], and a numerical solution technique using the finite element method (FEM) was discussed in [21]. One reason for studying wave propagation in this kind of device is that a waveguide is a better environment for measurements than a free-space arrangement, and that the analysis could be of use for the so called inverse problem of determining the material parameters of a chiral slab [16]. Results of such inverse experiments were reported in [2]. The closed bi-isotropic waveguide is a more general type of waveguide, consisting of one single, hollow, perfect conductor with bi-isotropic filling. A theory of time-harmonic wave propagation in closed and open bi-isotropic waveguides based on the wave-field concept is presented in Lindell *et al.* [14]. Basically, the wave fields are the same fields as those used in [15].

Pulse propagation in bi-isotropic waveguides, however, seems not to have been discussed. Such problems are complicated by material, anomalous, temporal dispersion in addition to dispersion caused by the presence of the waveguide [5, 12, 13, 17–19]. Pulse propagation in empty closed waveguides has been discussed by Kristensson using time-domain wave splitting [11], and Bernekorn *et al.* generalized the theory to waveguides with stratified, isotropic fillings using similar techniques [1]. In this article, the theory of pulse propagation in closed bi-isotropic waveguides is developed systematically using complex, time-dependent field vectors, see, *e.g.*, [3–5, 14, 20]. It is conjectured that the results can be used to solve inverse problems for bi-isotropic slabs using electromagnetic pulses, *c.f.* [2, 16]. By specialization, the technique in [1] for the homogeneous medium is improved. The complex fields correspond to the wave fields that have been used with success in the analysis of monochromatic wave propagation phenomena in linear bi-isotropic materials [14].

1.1   Notation

The radius vector is denoted by $\boldsymbol{r}$, the time by t, the electric and magnetic field vectors at $(\boldsymbol{r}, t)$ by $\boldsymbol{E}(\boldsymbol{r}, t)$ and $\boldsymbol{H}(\boldsymbol{r}, t)$, respectively, and the corresponding flux densities by $\boldsymbol{D}(\boldsymbol{r}, t)$ and $\boldsymbol{B}(\boldsymbol{r}, t)$. Each field vector is written in the form $\boldsymbol{E}(\boldsymbol{r}, t) = \boldsymbol{e}_x E_x(\boldsymbol{r}, t) + \boldsymbol{e}_y E_y(\boldsymbol{r}, t) + \boldsymbol{e}_z E_z(\boldsymbol{r}, t)$, where $\boldsymbol{e}_x$, $\boldsymbol{e}_y$, and $\boldsymbol{e}_z$ are the basis vectors in the

Cartesian frame. The dynamics of the fields is modeled by the macroscopic Maxwell equations: $\nabla \times \boldsymbol{E}(\boldsymbol{r}, t) = -\partial_t \boldsymbol{B}(\boldsymbol{r}, t)$ and $\nabla \times \boldsymbol{H}(\boldsymbol{r}, t) = \boldsymbol{J}(\boldsymbol{r}, t) + \partial_t \boldsymbol{D}(\boldsymbol{r}, t)$, where $\boldsymbol{J}(\boldsymbol{r}, t)$ is the current density at $(\boldsymbol{r}, t)$. For brevity, the independent variables $(\boldsymbol{r}, t)$ are often suppressed.

1.2 Constitutive relations

The constitutive relations of a linear, homogeneous, bi-isotropic material are given by $c_0 \eta_0 \boldsymbol{D} = \varepsilon \boldsymbol{E} + \xi \eta_0 \boldsymbol{H}$ and $c_0 \boldsymbol{B} = \zeta \boldsymbol{E} + \mu \eta_0 \boldsymbol{H}$, where the *relative* permittivity and permeability operators are $\varepsilon = 1 + \chi^{ee}(t)*$ and $\mu = 1 + \chi^{mm}(t)*$, the *relative* cross-coupling operators are $\xi = \chi^{em}(t)*$ and $\zeta = \chi^{me}(t)*$, and the asterisk $(*)$ denotes temporal convolution: $[\zeta \boldsymbol{E}](\boldsymbol{r}, t) = (\chi^{me} * \boldsymbol{E})(\boldsymbol{r}, t) = \int_{-\infty}^{t} \chi^{me}(t - t') \boldsymbol{E}(\boldsymbol{r}, t') \, dt'$. This is one of several proper ways to model the temporal dispersion of the bi-isotropic medium in the absence of a material optical response [8]. The constants c_0 and η_0 are the speed of light in vacuum and the intrinsic impedance of vacuum, respectively. The integral kernels $\chi^{ee}(t)$, $\chi^{em}(t)$, $\chi^{me}(t)$, and $\chi^{mm}(t)$ are the susceptibility kernels of the medium. Due to causality, the susceptibility kernels are identically zero for $t < 0$. For $t > 0$, they are assumed to be twice continuously differentiable. Pasteur media satisfy $\chi^{me}(t) = -\chi^{em}(t)$ and Tellegen materials $\chi^{me}(t) = \chi^{em}(t)$. In the short-wave limit, the constitutive relations reduce to the ones in vacuum provided that the susceptibility kernels are absolutely integrable. This is deduced from the Riemann-Lebesgue lemma. Furthermore, the continuity condition

$$\chi^{ee}(+0) = \chi^{em}(+0) = \chi^{mm}(+0) = \chi^{me}(+0) = 0. \tag{1.1}$$

is imposed on the isotropic chiral filling. This continuity condition implies that wave fronts propagate through the medium without attenuation or rotation. The condition $\chi^{ee}(+0) \neq 0$ is referred to as "unphysical" in a major textbook on classical electrodynamics [7]. The most often used model for bi-isotropic materials, Condon's (dispersion) model, satisfies $\chi^{ee}(+0) = 0$ but, unfortunately, $\chi^{em}(+0) \neq 0$ [5].

2 The complex electromagnetic fields

Substituting the constitutive relations into the Maxwell equations gives a linear system of first-order hyperbolic integro-differential equations in the electric and magnetic field vectors only:

$$\begin{cases} \nabla \times \boldsymbol{E} = -c_0^{-1} \partial_t \left(\zeta \boldsymbol{E} + \mu \eta_0 \boldsymbol{H} \right), \\ \nabla \times \eta_0 \boldsymbol{H} = \eta_0 \boldsymbol{J} + c_0^{-1} \partial_t \left(\varepsilon \boldsymbol{E} + \xi \eta_0 \boldsymbol{H} \right). \end{cases}$$

This system of equations can be decoupled by a linear transformation defined by

$$\begin{cases} \boldsymbol{E} = \boldsymbol{E}_+ + \boldsymbol{E}_-, \\ \eta_0 \boldsymbol{H} = i \mathcal{Y}_+ \boldsymbol{E}_+ - i \mathcal{Y}_- \boldsymbol{E}_-, \end{cases} \tag{2.1}$$

where i is the imaginary unit and the relative admittances $\mathcal{Y}_\pm = 1 + Y_\pm(t)*$ are complex-conjugated, temporal integral operators to be determined. The inverse of transformation (2.1) is given by

$$\boldsymbol{E}_\pm = (\mathcal{Y}_+ + \mathcal{Y}_-)^{-1} (\mathcal{Y}_\mp \boldsymbol{E} \mp i\eta_0 \boldsymbol{H}).$$

The complex fields $\boldsymbol{E}_\pm$ satisfy the linear system of first-order hyperbolic integro-differential equations

$$\begin{aligned}
\nabla \times \boldsymbol{E}_\pm = {}&\mp ic_0^{-1}\partial_t (\mathcal{Y}_+ + \mathcal{Y}_-)^{-1} (\mp i\mathcal{Y}_\mp (\zeta \boldsymbol{E} + \mu\eta_0 \boldsymbol{H}) + \varepsilon \boldsymbol{E} + \xi\eta_0 \boldsymbol{H}) \\
&\mp (\mathcal{Y}_+ + \mathcal{Y}_-)^{-1} i\eta_0 \boldsymbol{J} \\
= {}&\mp ic_0^{-1}\partial_t (\mathcal{Y}_+ + \mathcal{Y}_-)^{-1} (\varepsilon \mp i\mathcal{Y}_\mp \zeta + (\xi \mp i\mathcal{Y}_\mp\mu)i\mathcal{Y}_+) \boldsymbol{E}_+ \\
&\mp ic_0^{-1}\partial_t (\mathcal{Y}_+ + \mathcal{Y}_-)^{-1} (\varepsilon \mp i\mathcal{Y}_\mp \zeta - (\xi \mp i\mathcal{Y}_\mp\mu)i\mathcal{Y}_-) \boldsymbol{E}_- \\
&\mp (\mathcal{Y}_+ + \mathcal{Y}_-)^{-1} i\eta_0 \boldsymbol{J}.
\end{aligned}$$

Thus, the conditions on the relative admittances for decoupling are

$$\varepsilon \pm i\mathcal{Y}_\pm\zeta \pm (\xi \pm i\mathcal{Y}_\pm\mu)i\mathcal{Y}_\pm = 0, \tag{2.2}$$

with solutions

$$\mu\mathcal{Y}_\pm = \pm i\frac{\xi + \zeta}{2} + \mathcal{N},$$

where the real, temporal integral operator $\mathcal{N}$ is defined by[1]

$$\mathcal{N} = \sqrt{\mu\varepsilon - \frac{(\xi + \zeta)^2}{4}} = 1 + N^r(t) *.$$

The real kernel $N^r(t)$ satisfies the Volterra integral equation of the second kind

$$2N^r(t) + (N^r * N^r)(t) = \chi^{ee}(t) + \chi^{mm}(t) + (\chi^{ee} * \chi^{mm})(t) - (\chi * \chi)(t),$$

where $\chi(t) = \chi^{em}(t)/2 + \chi^{me}(t)/2$ is the nonreciprocity kernel. Volterra integral equations of the second kind are uniquely solvable in the space of of continuous functions in each compact time-interval and the solutions depend continuously on data [10]. Consequently, the kernel $N^r(t)$ inherits causality and smoothness properties from the susceptibility kernels. The admittance kernels can be written as $Y_\pm(t) = Y^r(t) \pm iY^i(t)$, where the components $Y^r(t)$ and $Y^i(t)$ are real functions. The admittance kernels satisfy the Volterra integral equation of the second kind

$$Y_\pm(t) + (Y_\pm * \chi^{mm})(t) = N^r(t) - \chi^{mm}(t) \pm i\chi(t).$$

In particular, the admittance kernels inherit causality and smoothness properties from the susceptibility kernels. Unique solubility gives that the admittance kernels of the bi-isotropic medium are real iff the medium is Pasteur, that is, $\chi(t) = 0$.

---

[1]The positive square-root-operator has been chosen. This choice is not of importance, since choosing the negative square-root-operator only implies that the complex fields $\boldsymbol{E}_\pm$ change roles.

As a consequence of (2.2), $(\mathcal{Y}_+ + \mathcal{Y}_-)^{-1} (\varepsilon \mp i\mathcal{Y}_\mp \zeta \pm (\xi \mp i\mathcal{Y}_\mp \mu)i\mathcal{Y}_\pm) = \mu\mathcal{Y}_\mp \pm i\xi$. Thus, the complex fields satisfy the first-order, dispersive vector wave equations

$$\nabla \times \boldsymbol{E}_\pm = \mp ic_0^{-1}\partial_t \mathcal{N}_\pm \boldsymbol{E}_\pm \mp i\mathcal{N}^{-1}\mu\eta_0 \boldsymbol{J}/2, \tag{2.3}$$

where the refractive indices $\mathcal{N}_\pm = 1 + N_\pm(t)*$ are complex-conjugated, temporal integral operators defined by

$$\mathcal{N}_\pm = \pm i\frac{\xi - \zeta}{2} + \mathcal{N}.$$

In terms of the kernel $N^r(t)$ and the chirality kernel $\kappa(t) = \chi^{em}(t)/2 - \chi^{me}(t)/2$, the complex refractive kernels are $N_\pm(t) = N^r(t) \pm iN^i(t) = N^r(t) \pm i\kappa(t)$. The refractive kernels are real iff the medium is Tellegen, that is, $\kappa(t) = 0$.

Equations (2.3) show that the complex fields $\boldsymbol{E}_\pm$ are independent. Having obtained these fields, the electric and magnetic fields are obtained from (2.1). It can happen that these linear combinations are found to be complex. *The real parts of the complex electric and magnetic fields are then solutions to the Maxwell equations*:

$$\begin{cases} \boldsymbol{E} = \mathrm{Re}\,(\boldsymbol{E}_+ + \boldsymbol{E}_-), \\ \eta_0 \boldsymbol{H} = \mathrm{Re}\,(i\mathcal{Y}_+ \boldsymbol{E}_+ - i\mathcal{Y}_- \boldsymbol{E}_-). \end{cases} \tag{2.4}$$

Without this simple but important observation, the number of possible solutions in, *e.g.*, waveguide problems is severely confined.

Notice that the continuity condition (1.1) implies that

$$N_\pm(+0) = Y_\pm(+0) = 0. \tag{2.5}$$

3 Pulse propagation in bi-isotropic waveguides

Consider a straight, cylindric waveguide extended in the z-direction. The interior of the guide is denoted by V and the boundary of the guide by S. The cross-section of the waveguide is denoted by Ω and the boundary of the cross-section by $\partial\Omega$. The reference direction of the normal vector field $\boldsymbol{n} = \boldsymbol{n}(\boldsymbol{r}_\perp)$ along $\partial\Omega$ is outward with respect to the bi-isotropic filling. The tangential vector field $\boldsymbol{\tau} = \boldsymbol{\tau}(\boldsymbol{r}_\perp)$ along $\partial\Omega$ is defined by $\boldsymbol{\tau} = \boldsymbol{n} \times \boldsymbol{e}_z$. The binormal vector field along $\partial\Omega$ is thus $\boldsymbol{e}_z$.

3.1 Decomposition into transverse and longitudinal fields

The complex fields are decomposed uniquely in transverse and longitudinal fields as is standard in waveguide theory: $\boldsymbol{E}_\pm = \boldsymbol{E}_{\pm,\perp} + \boldsymbol{e}_z E_{\pm,z}$. Similarly, the nabla operator is written $\nabla = \nabla_\perp + \boldsymbol{e}_z\partial_z$ and the Laplacian $\Delta = \Delta_\perp + \partial_z^2$. In the absence of sources, the first-order vector wave equations (2.3) for the complex fields are

$$\nabla \times \boldsymbol{E}_\pm = \mp i\mathcal{K}_\pm \boldsymbol{E}_\pm, \tag{3.1}$$

where $\mathcal{K}_\pm := c_0^{-1}\partial_t \mathcal{N}_\pm$. Alternatively,

$$\partial_z \boldsymbol{E}_{\pm,\perp} = \nabla_\perp E_{\pm,z} \pm i\mathcal{K}_\pm \, \boldsymbol{e}_z \times \boldsymbol{E}_{\pm,\perp}, \tag{3.2}$$

where $E_{\pm,z} = \mp i\mathcal{K}_\pm^{-1}\nabla_\perp \cdot \boldsymbol{e}_z \times \boldsymbol{E}_{\pm,\perp}$. Taking the curl of both members of (3.1) under consideration of $\nabla \cdot \boldsymbol{E}_\pm = 0$ gives second-order vector wave equations for the complex fields: $-\Delta \boldsymbol{E}_\pm = -\mathcal{K}_\pm^2 \boldsymbol{E}_\pm$. In particular, for the longitudinal component,

$$-\Delta E_{\pm,z} = -\mathcal{K}_\pm^2 E_{\pm,z}. \tag{3.3}$$

3.2 Modes of propagation

An up-going mode of propagation can be written formally as

$$\boldsymbol{E}_\pm \left(\boldsymbol{r}_\perp, z, t\right) = \exp\left(-zc_0^{-1}\partial_t \mathcal{N}_z\right)\boldsymbol{e}_\pm\left(\boldsymbol{r}_\perp, t\right), \tag{3.4}$$

where the complex, temporal integral operator $\mathcal{N}_z = 1 + N_z(t)*$ is referred to as the longitudinal index of refraction of the mode and the kernel N_z is causal. Observe that wave fronts travel along the axis of the guide with the speed of light in vacuum.

Equation (3.2) now reads $(-\mathcal{K}_z \mathbf{I}_{\perp\perp} \mp i\mathcal{K}_\pm \boldsymbol{e}_z \times \mathbf{I}_{\perp\perp}) \cdot \boldsymbol{e}_{\pm,\perp} = \nabla_\perp e_{\pm,z}$, where $\mathcal{K}_z := c_0^{-1}\partial_t \mathcal{N}_z$, and multiplying both members by $(-\mathcal{K}_z \mathbf{I}_{\perp\perp} \pm i\mathcal{K}_\pm \boldsymbol{e}_z \times \mathbf{I}_{\perp\perp})$ gives

$$\boldsymbol{e}_{\pm,\perp} = \left(\mathcal{K}_z^2 - \mathcal{K}^2\right)^{-1}\left(-\mathcal{K}_z \mathbf{I}_{\perp\perp} \pm i\mathcal{K}_\pm \boldsymbol{e}_z \times \mathbf{I}_{\perp\perp}\right) \cdot \nabla_\perp e_{\pm,z}. \tag{3.5}$$

Here $\boldsymbol{e}_\pm = \boldsymbol{e}_{\pm,\perp} + \boldsymbol{e}_z e_{\pm,z}$ and $\mathbf{I}_{\perp\perp} = \boldsymbol{e}_x \boldsymbol{e}_x + \boldsymbol{e}_y \boldsymbol{e}_y$. Equation (3.3) becomes

$$-\Delta_\perp e_{\pm,z} = \left(\mathcal{K}_z^2 - \mathcal{K}_\pm^2\right) e_{\pm,z}. \tag{3.6}$$

3.3 Propagators

The integral kernel $N_z(t)$ is supposed to inherit causality and regularity from the susceptibility kernels; in particular

$$N_z(+0) = 0. \tag{3.7}$$

Consequently, the propagator $\exp\left(-z\mathcal{K}_z\right) = \exp\left(-zc_0^{-1}\partial_t \mathcal{N}_z\right)$ can be factored as

$$\delta\left(t - zc_0^{-1}\right) * \exp\left(-zc_0^{-1}N_z'(t)*\right) = \delta\left(t - zc_0^{-1}\right) * \left(1 + P(z,t)*\right),$$

where the propagator kernel $P(z,t)$ satisfies the temporal Volterra integral equation

$$tP(z,t) = -tzc_0^{-1}N_z'(t) - \left(tzc_0^{-1}N_z' * P\right)(z,t) \tag{3.8}$$

in terms of the refractive kernel $N_z'(t)$. Propagators are well-known from one-dimensional propagation and scattering problems, see, *e.g.*, [9], where the integral equation (3.8) is solved for fixed $N_z(t)$. A more general discussion of functions of integral operators as $\exp\left(-z\mathcal{K}_z\right)$ can be found in the appendix.

3.4   Boundary conditions

At the boundary of the waveguide, $\boldsymbol{n} \times \boldsymbol{E} = \boldsymbol{0}$, i.e., $\boldsymbol{n} \times \boldsymbol{E}_+ + \boldsymbol{n} \times \boldsymbol{E}_- = \boldsymbol{0}$, $\boldsymbol{r} \in S$.

For a specific mode, the boundary conditions become ($\boldsymbol{\tau} = \boldsymbol{n} \times \boldsymbol{e}_z$)

$$\begin{cases} 0 = e_{+,z} + e_{-,z}, \\ 0 = (\mathcal{K}_z^2 - \mathcal{K}_+^2)^{-1}(-\mathcal{K}_z \partial_\tau e_{+,z} - i\mathcal{K}_+ \partial_n e_{+,z}) \qquad (\boldsymbol{r}_\perp \in \partial\Omega), \\ \quad + (\mathcal{K}_z^2 - \mathcal{K}_-^2)^{-1}(-\mathcal{K}_z \partial_\tau e_{-,z} + i\mathcal{K}_- \partial_n e_{-,z}) \end{cases} \qquad (3.9)$$

where the tangential and normal derivatives at the boundary are defined by $\partial_\tau e_{\pm,z} = \boldsymbol{\tau} \cdot \nabla_\perp e_{\pm,z}$ and $\partial_n e_{\pm,z} = \boldsymbol{n} \cdot \nabla_\perp e_{\pm,z} = -\boldsymbol{\tau} \cdot \boldsymbol{e}_z \times \nabla_\perp e_{\pm,z}$, respectively. The second condition unables time to be separated from the spatial variables.

3.5   Fundamental problem

The fundamental problem for the bi-isotropic waveguide is to determine the set of refractive indices such that equations (3.6) for the longitudinal fields subject to the boundary conditions (3.9) are solvable. The transverse fields are obtained from (3.5), and, finally, the complete time-domain propagation mode follows from (2.4) and (3.4):

$$\begin{cases} \boldsymbol{E}\,(\boldsymbol{r}_\perp, z, t) = \mathrm{Re}\,(\exp\,(-z\mathcal{K}_z)(\boldsymbol{e}_+\,(\boldsymbol{r}_\perp, t) + \boldsymbol{e}_-\,(\boldsymbol{r}_\perp, t))), \\ \eta_0 \boldsymbol{H}\,(\boldsymbol{r}_\perp, z, t) = \mathrm{Re}\,(\exp\,(-z\mathcal{K}_z)(i\mathcal{Y}_+ \boldsymbol{e}_+\,(\boldsymbol{r}_\perp, t) - i\mathcal{Y}_- \boldsymbol{e}_-\,(\boldsymbol{r}_\perp, t))). \end{cases} \qquad (3.10)$$

Observe that the longitudinal refractive indices appear in complex-conjugated pairs.

It is not possible to develop the general theory of the closed bi-isotropic waveguide further. For achiral waveguides (isotropic or Tellegen fillings), however, time can be separated from the spatial variables. This section is finished by presenting this theory. In sections 4 and 5, two special bi-isotropic waveguide geometries are analyzed.

3.5.1   Achiral guide

In the achiral guide, (3.6) becomes $-\Delta_\perp e_{\pm,z} = (\mathcal{K}_z^2 - \mathcal{K}^2)\,e_{\pm,z}$, where $\mathcal{K} = \mathcal{K}_+ = \mathcal{K}_-$. Since the boundary condition $e_{+,z} + e_{-,z} = 0$ implies that $\partial_\tau(e_{+,z} + e_{-,z}) = 0$, the second boundary condition (3.9) transforms into $\partial_n(e_{+,z} - e_{-,z}) = 0$, and the fundamental problem separates into a Dirichlet type of problem for the sum of $e_{+,z}$ and $e_{-,z}$ and a Neumann type of problem for the difference between $e_{+,z}$ and $e_{-,z}$. The two types of solutions are independent:

1. $e_{+,z}(\boldsymbol{r}_\perp, t) = e_{-,z}(\boldsymbol{r}_\perp, t) = v(\boldsymbol{r}_\perp)f(t)/2$, where the complex function $f(t)$ is arbitrary and the real function $v(\boldsymbol{r}_\perp)$ satisfies the Dirichlet problem

$$\begin{cases} -\Delta_\perp v(\boldsymbol{r}_\perp) = \lambda^2 v(\boldsymbol{r}_\perp) & (\boldsymbol{r}_\perp \in \Omega), \\ v(\boldsymbol{r}_\perp) = 0 & (\boldsymbol{r}_\perp \in \partial\Omega). \end{cases}$$

The longitudinal fields are

$$\begin{cases} E_z\left(\boldsymbol{r}_\perp, z, t\right) = \exp\left(-z\mathcal{K}_z\right)v(\boldsymbol{r}_\perp)\operatorname{Re} f(t), \\ \eta_0 H_z\left(\boldsymbol{r}_\perp, z, t\right) = \exp\left(-z\mathcal{K}_z\right)v(\boldsymbol{r}_\perp)\operatorname{Re}\left(i(\mathcal{Y}_+ - \mathcal{Y}_-)f(t)\right)/2. \end{cases}$$

These solutions reduce to TM solutions in the isotropic case, $\mathcal{Y}_+ = \mathcal{Y}_-$.

2. $e_{+,z}(\boldsymbol{r}_\perp, t) = -e_{-,z}(\boldsymbol{r}_\perp, t) = w(\boldsymbol{r}_\perp)g(t)/2$, where the complex function $g(t)$ is arbitrary and the real function $w(\boldsymbol{r}_\perp)$ satisfies the Neumann problem

$$\begin{cases} -\Delta_\perp w(\boldsymbol{r}_\perp) = \lambda^2 w(\boldsymbol{r}_\perp) & (\boldsymbol{r}_\perp \in \Omega), \\ \partial_n w(\boldsymbol{r}_\perp) = 0 & (\boldsymbol{r}_\perp \in \partial\Omega). \end{cases}$$

The longitudinal fields are the TE solutions

$$\begin{cases} E_z\left(\boldsymbol{r}_\perp, z, t\right) = 0, \\ \eta_0 H_z\left(\boldsymbol{r}_\perp, z, t\right) = \exp\left(-z\mathcal{K}_z\right)w(\boldsymbol{r}_\perp)\operatorname{Re}\left(i(\mathcal{Y}_+ + \mathcal{Y}_-)g(t)\right)/2. \end{cases}$$

In both cases, $\mathcal{K}_z^2 - \mathcal{K}^2 = \lambda^2 = \lambda^2\delta(t)*$, so that the longitudinal refractive kernel associated with λ is obtained by solving the Volterra equation of the second kind

$$2N_z(t) + (N_z * N_z)(t) - 2N(t) - (N * N)(t) = c_0^2\lambda^2 tH(t). \tag{3.11}$$

Equation (3.11) constitutes an improvement of the solution technique in [1].

3.5.2 The empty waveguide

In the empty waveguide, the kernel N in (3.11) is zero, and the longitudinal index of refraction can be computed exactly using the method of successive approximations. Setting $N_\perp(t) = c_0\lambda H(t)$ yields

$$N_z(t) = \sum_{k=1}^{\infty} \binom{\frac{1}{2}}{k} \left\{(N_\perp*)^{2k-1} N_\perp\right\}(t) = H(t)\sum_{k=1}^{\infty} \binom{\frac{1}{2}}{k} \frac{(c_0\lambda)^{2k}}{(2k-1)!}t^{2k-1} =$$

$$= H(t)\int_0^t \left\{\sum_{k=1}^{\infty} \frac{(-1)^{k-1}}{(2k)!!} \frac{(c_0\lambda)^{2k}}{(2k-2)!!}t^{2k-2}\right\} dt = H(t)\int_0^t \frac{c_0\lambda}{t}J_1(c_0\lambda t)\,dt,$$

where a Bessel function expansion (A.4) has been used. This result was derived in [11] using a different technique. Notice that the result is in accord with (3.7).

4 Circular bi-isotropic waveguide

The polar coordinates are denoted by ρ, ϕ, i.e., $x = \rho\cos\phi$ and $y = \rho\sin\phi$. For a waveguide of circular cross-section of radius a, $\Omega = \{(x, y) : \rho < a\}$, set

$$e_{\pm,z}\left(\boldsymbol{r}_\perp, t\right) = J_n\left(\rho\sqrt{\mathcal{K}_z^2 - \mathcal{K}_\pm^2}\right)\exp\left(-in\phi\right)f_\pm(t) \qquad (\rho < a), \tag{4.1}$$

where J_n is a Bessel function of the first kind and integer order n and $f_\pm = f_\pm(t)$ are complex functions. The functions of integral operators present in (4.1) and in (4.2) below are defined in the appendix and in Section 4.1.

Since $\partial_\tau = -a^{-1}\partial_\phi$ and $\partial_n = \partial_\rho$, the boundary conditions give the system of integral equations

$$\begin{pmatrix} J_n\left(a\sqrt{\mathcal{K}_z^2 - \mathcal{K}_+^2}\right) & J_n\left(a\sqrt{\mathcal{K}_z^2 - \mathcal{K}_-^2}\right) \\ \mathcal{A}_+ & \mathcal{A}_- \end{pmatrix} \begin{pmatrix} f_+ \\ f_- \end{pmatrix} = \begin{pmatrix} 0 \\ 0 \end{pmatrix},$$

where

$$\mathcal{A}_\pm = -\left(\mathcal{K}_z^2 - \mathcal{K}_\pm^2\right)^{-1}\mathcal{K}_z(a^{-1}in)J_n\left(a\sqrt{\mathcal{K}_z^2 - \mathcal{K}_\pm^2}\right)$$

$$\mp i\mathcal{K}_\pm\left(\mathcal{K}_z^2 - \mathcal{K}_\pm^2\right)^{-1/2}J_n'\left(a\sqrt{\mathcal{K}_z^2 - \mathcal{K}_\pm^2}\right).$$

The condition $J_n\left(a\sqrt{\mathcal{K}_z^2 - \mathcal{K}_+^2}\right)\mathcal{A}_- - J_n\left(a\sqrt{\mathcal{K}_z^2 - \mathcal{K}_-^2}\right)\mathcal{A}_+ = 0$ for non-trivial solutions becomes

$$-\frac{n}{a}\left(\left(\mathcal{K}_z^2 - \mathcal{K}_-^2\right)^{-1} - \left(\mathcal{K}_z^2 - \mathcal{K}_+^2\right)^{-1}\right)\mathcal{K}_z J_n\left(a\sqrt{\mathcal{K}_z^2 - \mathcal{K}_-^2}\right) J_n\left(a\sqrt{\mathcal{K}_z^2 - \mathcal{K}_+^2}\right)$$

$$+ \mathcal{K}_-\left(\mathcal{K}_z^2 - \mathcal{K}_-^2\right)^{-1/2}J_n'\left(a\sqrt{\mathcal{K}_z^2 - \mathcal{K}_-^2}\right) J_n\left(a\sqrt{\mathcal{K}_z^2 - \mathcal{K}_+^2}\right)$$

$$+ \mathcal{K}_+\left(\mathcal{K}_z^2 - \mathcal{K}_+^2\right)^{-1/2}J_n'\left(a\sqrt{\mathcal{K}_z^2 - \mathcal{K}_+^2}\right) J_n\left(a\sqrt{\mathcal{K}_z^2 - \mathcal{K}_-^2}\right) = 0. \tag{4.2}$$

This dispersion equation is in concordance with the fixed frequency result (4.78) in Lindell. Complex conjugation shows that $\mathcal{K}_z \neq \mathcal{K}_z^*$ unless $n = 0$ (or $\mathcal{K}_+ = \mathcal{K}_-$).

4.1 Analysis of the dispersion equation

Due to the continuity conditions (2.5) and (3.7), the square-root operators of interest are of the form

$$a\sqrt{\mathcal{K}_z^2 - \mathcal{K}_\pm^2} = \sqrt{\lambda_z - \lambda_\pm} + U_\pm(t)*, \tag{4.3}$$

where

$$\lambda_i = 2a^2 c_0^{-2} N_i'(+0) \qquad (i = +, -, z), \tag{4.4}$$

are dimensionless numbers and the kernels $U_\pm$ satisfy the equations

$$2\sqrt{\lambda_z - \lambda_\pm}U_\pm(t) + (U_\pm * U_\pm)(t) = (\lambda_z - \lambda_\pm)(N_z(t) + N_\pm(t))/2$$
$$+ \left[2(N_z''(t) - N_\pm''(t)) + ((N_z'' - N_\pm'') * (N_z + N_\pm))(t)\right]\left(ac_0^{-1}\right)^2. \tag{4.5}$$

Since, by definition, $N_z(t) = (H * N_z')(t)$, and, consequently,

$$\begin{cases} N_z'(t) = N_z'(+0)H(t) + (H * N_z'')(t), \\ N_z(t) = N_z'(+0)tH(t) + ((tH) * N_z'')(t), \end{cases} \tag{4.6}$$

equations (4.5) are temporal Volterra integral equations of the second kind in the unknown kernels $U_\pm(t)$ and $N_z''(t)$ for a fixed value of $\lambda_z = 2a^2 c_0^{-2} N_z'(+0)$.

The Bessel functions operators are given by

$$\begin{cases} J_n\left(\rho\sqrt{\mathcal{K}_z^2 - \mathcal{K}_\pm^2}\right) = J_n\left(\rho/a\sqrt{\lambda_z - \lambda_\pm}\right) + V_{\pm,n}(\rho, t)*, \\ J_n'\left(\rho\sqrt{\mathcal{K}_z^2 - \mathcal{K}_\pm^2}\right) = J_n'\left(\rho/a\sqrt{\lambda_z - \lambda_\pm}\right) + W_{\pm,n}(\rho, t)* \end{cases} \tag{4.7}$$

where the kernels $V_{\pm,n}(\rho, t)$ and $W_{\pm,n}(\rho, t)$ for fixed ρ satisfy the temporal Volterra integral equations of the second kind

$$\begin{aligned} &(\rho/a)^2 \left(\sqrt{\lambda_z - \lambda_\pm} + U_\pm(t)*\right)^2 (tW_{\pm,n}(\rho, t)) \\ &+ \rho/a \left(\sqrt{\lambda_z - \lambda_\pm} + U_\pm(t)*\right) (tV_{\pm,n}(\rho, t)) \\ &+ \left((\rho/a)^2 \left(\sqrt{\lambda_z - \lambda_\pm} + U_\pm(t)*\right)^2 - n^2\right) \\ &\left(J_n\left(\rho/a\sqrt{\lambda_z - \lambda_\pm}\right) + V_{\pm,n}(\rho, t)*\right) (t\rho a^{-1} U_\pm(t)) = 0, \end{aligned} \tag{4.8}$$

where

$$tV_{\pm,n}(\rho, t) = \left(J_n'\left(\rho/a\sqrt{\lambda_z - \lambda_\pm}\right) + W_{\pm,n}(\rho, t)*\right) (t\rho a^{-1} U_\pm(t)) \tag{4.9}$$
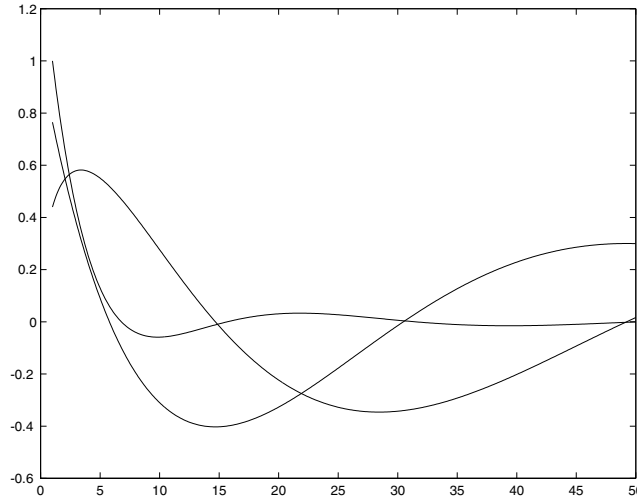
in terms of the kernels $U_\pm(t)$.

If now the operators (4.3) and (4.7) (with $\rho = a$) are substituted into the dispersion equation (4.2), the thus obtained equation and equations (4.5), (4.8), and (4.9) (with $\rho = a$) constitute a system of seven coupled Volterra integral equations of the second kind in the seven kernels $N_z''(t)$, $U_\pm(t)$, $V_{\pm,n}(a, t)$, and $W_{\pm,n}(a, t)$. Solving these equations simultaneously determines the modes of propagation. Since Volterra integral equations of the second kind are stable, good results can be anticipated.

4.2   Variety of modes

So far the variety of modes pf propagation has not been considered. Matching the principal parts in the dispersion equation (4.2) gives the transcendental equation

$$\begin{aligned} &- n\left((\lambda_z - \lambda_-)^{-1} - (\lambda_z - \lambda_+)^{-1}\right) J_n\left(\sqrt{\lambda_z - \lambda_-}\right) J_n\left(\sqrt{\lambda_z - \lambda_+}\right) \\ &+ (\lambda_z - \lambda_-)^{-1/2} J_n'\left(\sqrt{\lambda_z - \lambda_-}\right) J_n\left(\sqrt{\lambda_z - \lambda_+}\right) \\ &+ (\lambda_z - \lambda_+)^{-1/2} J_n'\left(\sqrt{\lambda_z - \lambda_+}\right) J_n\left(\sqrt{\lambda_z - \lambda_-}\right) = 0. \end{aligned} \tag{4.10}$$

Figure 1: The functions $f(\lambda_z)$ in (4.11), $J_0(\sqrt{\lambda_z})$, and $J_1(\sqrt{\lambda_z})$ restricted to the interval $1 < \lambda_z < 50$ when $\lambda_\pm = 1 \pm i/10$. The four (visible) zeros of $f(\lambda_z)$ are close to the two (visible) zeros of $J_0(\sqrt{\lambda_z})$ and the two (visible) zeros of $J_1(\sqrt{\lambda_z})$.

The complex roots of this equation, λ_z, determine the modes. For $n = 0$, one gets

$$
\begin{aligned}
f(\lambda_z) &:= (\lambda_z - \lambda_-)^{-1/2} J_1\left(\sqrt{\lambda_z - \lambda_-}\right) J_0\left(\sqrt{\lambda_z - \lambda_+}\right) \\
&+ (\lambda_z - \lambda_+)^{-1/2} J_1\left(\sqrt{\lambda_z - \lambda_+}\right) J_0\left(\sqrt{\lambda_z - \lambda_-}\right) = 0
\end{aligned}
\tag{4.11}
$$

using the identity $J_0'(z) = -J_1(z)$. For $n > 0$, one obtains

$$
\begin{aligned}
&- (\lambda_z - \lambda_-)^{-1/2} J_{n+1}\left(\sqrt{\lambda_z - \lambda_-}\right) J_n\left(\sqrt{\lambda_z - \lambda_+}\right) \\
&+ (\lambda_z - \lambda_+)^{-1/2} J_{n-1}\left(\sqrt{\lambda_z - \lambda_+}\right) J_n\left(\sqrt{\lambda_z - \lambda_-}\right) = 0
\end{aligned}
$$

using the identities $J_n'(z) = \mp J_{n\pm1}(z) \pm nJ_n(z)/z$.

If $\lambda_+ = \lambda_- := \lambda$, equation (4.10) simplifies to $J_n'\left(\sqrt{\lambda_z - \lambda}\right) J_n\left(\sqrt{\lambda_z - \lambda}\right) = 0$ with solutions $\lambda_z = \lambda + \xi_{nk}^2$ and $\lambda_z = \lambda + \eta_{nk}^2$, where ξ_{nk} and η_{nk} are the zeros of $J_n(x)$ and $J_n'(x)$, respectively. Consequently, there are infinitely many roots in this (constructed) case. Since the imaginary parts of $\lambda_\pm$ can be anticipated to be small compared to the real part, a similar behavior is expected in the case $\lambda_+ \neq \lambda_-$. In Figure 1, the function $f(\lambda_z)$ in the left member of (4.11) is plotted in the interval $1 < \lambda_z < 50$ when $\lambda_\pm = 1 \pm i/10$. Observe that $f(\lambda_z)$ is real on the real axis.

4.3 Determination of a specific mode

Once a value of $\lambda_z = 2a^2 c_0^{-2} N_z'(+0)$ has been determined, one proceeds by solving a system of Volterra interval equations of the second kind as described in Section 4.1. This procedure gives the kernel $N_z''(t)$. Since $N_z'(+0)$ is known, the kernel $N_z'(t)$ can be obtained by straightforward integration, see (4.6). In this way, the longitudinal refractive kernel $N_z(t)$ characterizing the mode is obtained.

In the procedure, the kernels $U_{\pm}(t)$ present in (4.3) have been obtained as well. Using these kernels, the kernels $V_{\pm,n}(\rho, t)$ and $W_{\pm,n}(\rho, t)$ in (4.7) for any $\rho < a$ can be determined by solving the four Volterra interval equations of the second kind, that (4.8) and (4.9) constitute, simultaneously. This gives the longitudinal fields $e_{\pm,z}(\boldsymbol{r}_{\perp}, t)$ in (4.1), whereupon the transverse fields $\boldsymbol{e}_{\pm,\perp}(\boldsymbol{r}_{\perp}, t)$ can be calculated using (3.5). Finally, the electric and magnetic fields associated with the mode can be computed using (3.10).

4.4   Achiral limit

In the achiral limit, $\mathcal{K}_+ = \mathcal{K}_-$, one gets the expected solutions:

$$\begin{cases} J_n\left(a\sqrt{\mathcal{K}_z^2 - \mathcal{K}^2}\right) = 0 \implies a\sqrt{\mathcal{K}_z^2 - \mathcal{K}^2} = \xi_{nk}\delta(t)* \implies f_+ - f_- = 0, \\ J_n'\left(a\sqrt{\mathcal{K}_z^2 - \mathcal{K}^2}\right) = 0 \implies a\sqrt{\mathcal{K}_z^2 - \mathcal{K}^2} = \eta_{nk}\delta(t)* \implies f_+ + f_- = 0. \end{cases}$$

The upper condition gives TM pulses (see equation (3.10)),

$$\begin{cases} E_z(\boldsymbol{r}_{\perp}, z, t) = \exp(-z\mathcal{K}_z)J_n(\rho/a\xi_{nk})\, 2\,\mathrm{Re}\left(\exp(-in\phi)f_+(t)\right), \\ \eta_0 H_z(\boldsymbol{r}_{\perp}, z, t) = 0, \end{cases} \qquad (\rho < a),$$

and the lower condition represents TE pulses,

$$\begin{cases} E_z(\boldsymbol{r}_{\perp}, z, t) = 0, \\ \eta_0 H_z(\boldsymbol{r}_{\perp}, z, t) = \exp(-z\mathcal{K}_z)\mathcal{Y}J_n(\rho/a\eta_{nk})\, 2\,\mathrm{Re}\left(i\exp(-in\phi)f_+(t)\right), \end{cases} \qquad (\rho < a).$$

5   Bi-isotropic parallel-plate waveguide

The cross-section of the parallel-plate waveguide is defined by $\Omega = \{(x,y) : |y| < d/2\}$. There are two kinds of solutions, namely odd (w.r.t. y) longitudinal fields and even (w.r.t. y) longitudinal fields.

5.1   Odd longitudinal fields

For odd longitudinal fields, one has

$$e_{\pm,z}(\boldsymbol{r}_{\perp}, t) = \sin\left(y\sqrt{\mathcal{K}_z^2 - \mathcal{K}_{\pm}^2}\right)f_{\pm}(t) \qquad (|y| < d/2),$$

where $f_{\pm} = f_{\pm}(t)$ are complex functions, $d/2\sqrt{\mathcal{K}_z^2 - \mathcal{K}_{\pm}^2} = \sqrt{\lambda_z - \lambda_{\pm}} + U_{\pm}(t)*$, $\lambda_i = d^2 c_0^{-2} N_i'(+0)/2$ for $i = \pm$ and $i = z$, and the kernels $U_{\pm}(t)$ satisfy (4.5) with a

substituted for $d/2$. The sine and cosine operators are defined in the appendix:

$$\begin{cases} \sin\left(y\sqrt{\mathcal{K}_z^2 - \mathcal{K}_\pm^2}\right) = \sin\left(2y/d\sqrt{\lambda_z - \lambda_\pm}\right) + V_\pm(y,t)*, \\ \cos\left(y\sqrt{\mathcal{K}_z^2 - \mathcal{K}_\pm^2}\right) = \cos\left(2y/d\sqrt{\lambda_z - \lambda_\pm}\right) + W_\pm(y,t)*, \end{cases}$$

where the kernels $V_\pm(y,t)$ and $W_\pm(y,t)$ for fixed y satisfy the temporal Volterra integral equations of the second kind

$$\begin{cases} tV_\pm(y,t) = 2y/d\cos\left(2y/d\sqrt{\lambda_z - \lambda_\pm}\right)tU_\pm(t) + 2y/dW_\pm(y,t)*(tU_\pm(t)), \\ -tW_\pm(y,t) = 2y/d\sin\left(2y/d\sqrt{\lambda_z - \lambda_\pm}\right)tU_\pm(t) + 2y/dV_\pm(y,t)*(tU_\pm(t)). \end{cases}$$

The boundary conditions yield the system of integral equations

$$\begin{pmatrix} \sin\left(d/2\sqrt{\mathcal{K}_z^2 - \mathcal{K}_+^2}\right) & \sin\left(d/2\sqrt{\mathcal{K}_z^2 - \mathcal{K}_-^2}\right) \\ \mathcal{A}_+ & \mathcal{A}_- \end{pmatrix}\begin{pmatrix} f_+ \\ f_- \end{pmatrix} = \begin{pmatrix} 0 \\ 0 \end{pmatrix},$$

where $\mathcal{A}_\pm = \mp i\mathcal{K}_\pm(\mathcal{K}_z^2 - \mathcal{K}_\pm^2)^{-1/2}\cos\left(d/2\sqrt{\mathcal{K}_z^2 - \mathcal{K}_\pm^2}\right)$. The condition for non-trivial solutions becomes

$$\begin{cases} \sin\left(d/2\sqrt{\mathcal{K}_z^2 - \mathcal{K}_+^2}\right)\mathcal{K}_-(\mathcal{K}_z^2 - \mathcal{K}_-^2)^{-1/2}\cos\left(d/2\sqrt{\mathcal{K}_z^2 - \mathcal{K}_-^2}\right) \\ + \sin\left(d/2\sqrt{\mathcal{K}_z^2 - \mathcal{K}_-^2}\right)\mathcal{K}_+(\mathcal{K}_z^2 - \mathcal{K}_+^2)^{-1/2}\cos\left(d/2\sqrt{\mathcal{K}_z^2 - \mathcal{K}_+^2}\right) = 0. \end{cases}$$

Modes are obtained using the same method as was sketched for the circular guide. Seven Volterra integral equations of the second kind are to be solved simultaneously.

The principal part of the dispersion equation is

$$\begin{aligned} g(\lambda_z) &:= (\lambda_z - \lambda_-)^{-1/2}\cos\left(\sqrt{\lambda_z - \lambda_-}\right)\sin\left(\sqrt{\lambda_z - \lambda_+}\right) \\ &+ (\lambda_z - \lambda_+)^{-1/2}\cos\left(\sqrt{\lambda_z - \lambda_+}\right)\sin\left(\sqrt{\lambda_z - \lambda_-}\right) = 0 \end{aligned} \tag{5.1}$$

In Figure 2, the function $g(\lambda_z)$ in the left member of (5.1) is plotted in the real interval $1 < \lambda_z < 50$ when $\lambda_\pm = 1 \pm i/10$.

In the achiral limit, $\mathcal{K}_+ = \mathcal{K}_-$, one gets the expected solutions:

$$\begin{cases} \sin\left(d/2\sqrt{\mathcal{K}_z^2 - \mathcal{K}^2}\right) = 0 \implies d/2\sqrt{\mathcal{K}_z^2 - \mathcal{K}^2} = n\pi\delta(t)* \implies f_+ - f_- = 0, \\ \cos\left(d/2\sqrt{\mathcal{K}_z^2 - \mathcal{K}^2}\right) = 0 \implies d/2\sqrt{\mathcal{K}_z^2 - \mathcal{K}^2} = (n+1/2)\pi\delta(t)* \implies f_+ + f_- = 0. \end{cases}$$
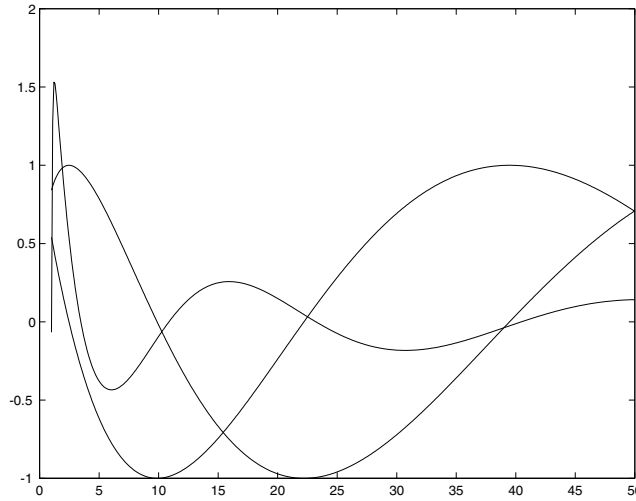
The upper condition gives the TM pulses (see equation (3.10)),

$$E_z(\boldsymbol{r}_\perp, z, t) = \exp(\mp z\mathcal{K}_z)\sin(2\pi ny/d)2\operatorname{Re}(f_+(t)) \qquad (|y| < d/2),$$

and the lower condition represents the TE pulses,

$$\eta_0 H_z(\boldsymbol{r}_\perp, z, t) = \exp(\mp z\mathcal{K}_z)\mathcal{Y}\sin(2\pi(n+1/2)y/d)2\operatorname{Re}(if_+(t)) \qquad (|y| < d/2).$$

Figure 2: The functions $g(\lambda_z)$ in (5.1), $\sin(\sqrt{\lambda_z})$, and $\cos(\sqrt{\lambda_z})$.

5.2 Even longitudinal fields

For even longitudinal fields, one has

$$e_{\pm,z}(\boldsymbol{r}_\perp,t) = \cos\left(y\sqrt{\mathcal{K}_z^2 - \mathcal{K}_\pm^2}\right) f_\pm(t) \qquad (|y| < d/2),$$

which yields the dispersion equation

$$\begin{cases} \cos\left(d/2\sqrt{\mathcal{K}_z^2 - \mathcal{K}_+^2}\right)\mathcal{K}_-(\mathcal{K}_z^2 - \mathcal{K}_-^2)^{-1/2}\sin\left(d/2\sqrt{\mathcal{K}_z^2 - \mathcal{K}_-^2}\right) \\ + \cos\left(d/2\sqrt{\mathcal{K}_z^2 - \mathcal{K}_-^2}\right)\mathcal{K}_+(\mathcal{K}_z^2 - \mathcal{K}_+^2)^{-1/2}\sin\left(d/2\sqrt{\mathcal{K}_z^2 - \mathcal{K}^2}\right) = 0 \end{cases}$$

with principal part

$$\begin{aligned} h(\lambda_z) &:= (\lambda_z - \lambda_-)^{-1/2}\sin\left(\sqrt{\lambda_z - \lambda_-}\right)\cos\left(\sqrt{\lambda_z - \lambda_+}\right) \\ &+ (\lambda_z - \lambda_+)^{-1/2}\sin\left(\sqrt{\lambda_z - \lambda_+}\right)\cos\left(\sqrt{\lambda_z - \lambda_-}\right) = 0. \end{aligned} \tag{5.2}$$

The dispersion equation is solved on the same way as in the previous section. Note the similarity between (4.11) and (5.2). In Figure 3, the function $h(\lambda_z)$ in the left member of (5.2) is plotted in the real interval $1 < \lambda_z < 50$ when $\lambda_\pm = 1 \pm i/10$.

Appendix A   Functions of convolution operators

In this appendix some functions of causal convolution operators are defined and convolution equations for these functions derived.

If c is complex constant and if $C(t)$ is a complex function that vanishes for $t < 0$ and is bounded and continuous for $t < 0$, then $\mathcal{C} = c + C(t)* = (c\delta(t) + C(t)) *$ is
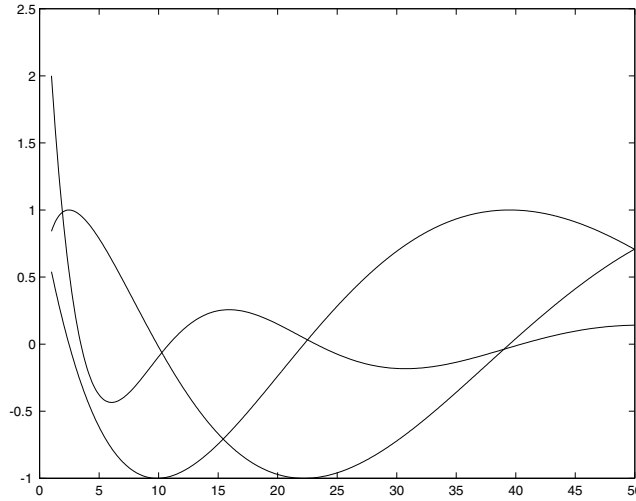
Figure 3: The functions $h(\lambda_z)$ in (5.2), $\sin(\sqrt{\lambda_z})$, and $\cos(\sqrt{\lambda_z})$.

said to be a causal convolution operator with the kernel $c\delta(t) + C(t)$. The operator $\mathcal{C}$ is said to be of the first kind if $c = 0$; otherwise, it is of the second kind.

Recall the simple facts that convolution is commutative and that causal convolution is associative. Among the causal convolution operators, there exists a causal convolution operator of the second kind, referred to as the identity operator and denoted by $\mathcal{I} = \delta(t)*$, with the property that $\mathcal{I}\mathcal{C} = \mathcal{C}$ for each causal convolution operator $\mathcal{C}$ of the first or of the second kind. To each causal convolution operator $\mathcal{C}$ of the second kind, there is a causal convolution operator of the second kind, referred to as the inverse of $\mathcal{C}$ and denoted by $\mathcal{C}^{-1}$, with the property that $\mathcal{C}\mathcal{C}^{-1} = \mathcal{I}$. By introducing $F(z) = z^{-1}$, one has $\mathcal{C}F(\mathcal{C}) = \mathcal{I}$ and $F(\mathcal{C}) = F(c) + F_{\mathcal{C}}(t)*$, where

$$cF_{\mathcal{C}}(t) + F(c)C(t) + F_{\mathcal{C}}(t) * C(t) = 0. \tag{A.1}$$

The inverse of $\mathcal{C}$ can also be written explicitly as

$$\mathcal{C}^{-1} = c^{-1}\left(1 + \frac{C(t)}{c}*\right)^{-1} = c^{-1} + c^{-1}\sum_{n=1}^{\infty}(-1)^n\left(\frac{C(t)}{c}*\right)^n,$$

where the series converges uniformly in each bounded interval. The set of kernels of causal convolution operators of the second kind and the convolution operation $*$ constitute an Abelian group, a fact that often, tacitly, will be used below. Unless stated otherwise, $\mathcal{C}$ will denote a given second-kind causal convolution operator.

A.1 Entire functions

Let $F(z)$ be an entire function, let $f(z) = F'(z)$ be the derivative of $F(z)$, and define

$$\begin{cases} F(\mathcal{C}) = \displaystyle\sum_{n=0}^{\infty} F_n \mathcal{C}^n, \\[2mm] f(\mathcal{C}) = F'(\mathcal{C}) = \displaystyle\sum_{n=0}^{\infty} n F_n \mathcal{C}^{n-1}, \end{cases}$$

where the complex numbers F_n are the coefficients in the Taylor expansion of $F(z)$:

$$F(z) = \sum_{n=0}^{\infty} F_n z^n.$$

Then $F(\mathcal{C})$ and $f(\mathcal{C})$ are causal convolution operators of the form

$$\begin{cases} F(\mathcal{C}) = F(c) + F_{\mathcal{C}}(t)* = (F(c)\delta(t) + F_{\mathcal{C}}(t)) *, \\ f(\mathcal{C}) = f(c) + f_{\mathcal{C}}(t)* = (f(c)\delta(t) + f_{\mathcal{C}}(t)) *, \end{cases}$$

where the causal kernels $F_{\mathcal{C}}(t)$ and $f_{\mathcal{C}}(t)$ are related as

$$t F_{\mathcal{C}}(t) = f(c) t C(t) + f_{\mathcal{C}}(t) * (t C(t)). \tag{A.2}$$

For use of $t\delta(t) = 0$ and $t(U(t) * V(t)) = (tU(t)) * V(t) + U(t) * (tV(t))$ gives

$$t \left(\sum_{n=0}^{\infty} F_n \mathcal{C}^n \delta(t) \right) = \sum_{n=0}^{\infty} n F_n \mathcal{C}^{n-1} \left(t \left(\mathcal{C}\delta(t) \right) \right),$$

that is,

$$t \left(F(\mathcal{C})\delta(t) \right) = F'(\mathcal{C}) \left(t \left(\mathcal{C}\delta(t) \right) \right), \tag{A.3}$$

which is equivalent to the wanted formula. Observe that $\mathcal{C}$ may be of the first kind.

A.2 Exponential, sine, and cosine functions

Equation (A.2) applies to the exponential function, $F(z) = \exp(z) = f(z)$:

$$t F_{\mathcal{C}}(t) = \exp(c) t C(t) + F_{\mathcal{C}}(t) * (t C(t)).$$

Moreover, it applies to the sine and cosine functions. If $F(z) = \sin(z)$ and $G(z) = \cos(z)$, then $f(z) = G(z)$ and $g(z) = -F(z)$, and equation (A.3) gives two Volterra integral equations of the second kind to be solved simultaneously:

$$\begin{cases} t F_{\mathcal{C}}(t) = \cos(c) t C(t) + G_{\mathcal{C}}(t) * (t C(t)), \\ -t G_{\mathcal{C}}(t) = \sin(c) t C(t) + F_{\mathcal{C}}(t) * (t C(t)). \end{cases}$$

A.3 Bessel functions

Since the Bessel functions

$$J_n(z) = \left(\frac{z}{2}\right)^n \sum_{j=0}^{\infty} (-1)^j \frac{1}{j!(n+j)!} \left(\frac{z}{2}\right)^{2j} \tag{A.4}$$

of the first kind and integer order are entire functions, (A.3) can be applied to their first derivatives:

$$t\left(F'(\mathcal{C})\delta(t)\right) = F''(\mathcal{C})\left(t\left(\mathcal{C}\delta(t)\right)\right). \tag{A.5}$$

Combining (A.3) and (A.2) with the Bessel equation

$$z^2 J_n''(z) + z J_n'(z) + \left(z^2 - n^2\right) J_n(z) = 0$$

gives useful identities. Operating with $\mathcal{C}^2 j_n'(\mathcal{C}) + \mathcal{C} J_n'(\mathcal{C}) + (\mathcal{C}^2 - n^2) J_n(\mathcal{C}) = 0$ on the function $t\left(\mathcal{C}\delta(t)\right) = tC(t)$ — recall the notation $j_n(z) = J_n'(z)$ — results in

$$\begin{cases} \mathcal{C}^2\left(t\left(j_n(\mathcal{C})\delta(t)\right)\right) + \mathcal{C}\left(t\left(J_n(\mathcal{C})\delta(t)\right)\right) + \left(\mathcal{C}^2 - n^2\right) J_n(\mathcal{C})\left(t\left(\mathcal{C}\delta(t)\right)\right) = 0, \\ t\left(J_n(\mathcal{C})\delta(t)\right) = j_n(\mathcal{C})\left(t\left(\mathcal{C}\delta(t)\right)\right), \end{cases}$$

which, since

$$\begin{cases} J_n(\mathcal{C}) = J_n(c) + J_{n\mathcal{C}}(t)* = \left(J_n(c)\delta(t) + J_{n\mathcal{C}}(t)\right)*, \\ j_n(\mathcal{C}) = j_n(c) + j_{n\mathcal{C}}(t)* = \left(j_n(c)\delta(t) + j_{n\mathcal{C}}(t)\right)* \end{cases}$$

constitutes a system of convolution equations in the kernels $J_{n\mathcal{C}}(t)$ and $j_{n\mathcal{C}}(t)$:

$$\begin{cases} (c + C(t)*)^2\left(tj_{n\mathcal{C}}(t)\right) + (c + C(t)*)\left(tJ_{n\mathcal{C}}(t)\right) \\ \quad + \left((c + C(t)*)^2 - n^2\right)\left(J_n(c) + J_{n\mathcal{C}}(t)*\right)\left(tC(t)\right) = 0, \\ tJ_{n\mathcal{C}}(t) = \left(j_n(c) + j_{n\mathcal{C}}(t)*\right)\left(tC(t)\right). \end{cases}$$

References

[1] P. Bernekorn, A. Karlsson, and G. Kristensson. Propagation of transient electromagnetic waves in inhomogeneous and dispersive waveguides. *J. Electro. Waves Applic.*, **10**(9), 1263–1286, 1996.

[2] G. Busse, J. Reinert, and A. F. Jacob. Waveguide Characterization of Chiral Material: Experiments. *IEEE Trans. Microwave Theory Tech.*, **47**(3), 297–301, 1999.

[3] I. Egorov, A. Karlsson, and S. Rikte. Corrigendum to [4]. *J. Phys. A: Math. Gen.*, **31**(22), 5191, June 1998.

[4] I. Egorov, A. Karlsson, and S. Rikte. Time-domain Green dyadics for temporally dispersive, simple media. *J. Phys. A: Math. Gen.*, **31**(14), 3219–3240, 1998. See [3] for corrections.

[5] I. Egorov and S. Rikte. Forerunners in bigyrotropic materials. *J. Opt. Soc. Am. A*, **15**(9), 2391–2403, 1998.

[6] R. Hollinger, V. V. Varadan, and V. K. Varadan. Eigenmodes in a circular waveguide containing an isotropic chiral material. *Radio Sci.*, **26**(5), 1335–1344, 1991.

[7] J. D. Jackson. *Classical Electrodynamics*. John Wiley & Sons, New York, second edition, 1975.

[8] A. Karlsson and G. Kristensson. Constitutive relations, dissipation and reciprocity for the Maxwell equations in the time domain. *J. Electro. Waves Applic.*, **6**(5/6), 537–551, 1992.

[9] A. Karlsson and S. Rikte. The time-domain theory of forerunners. *J. Opt. Soc. Am. A*, **15**(2), 487–502, 1998.

[10] R. Kress. *Linear Integral Equations*. Springer-Verlag, Berlin Heidelberg, 1989.

[11] G. Kristensson. Transient electromagnetic wave propagation in waveguides. *J. Electro. Waves Applic.*, **9**(5/6), 645–671, 1995.

[12] G. Kristensson and S. Rikte. Scattering of transient electromagnetic waves in reciprocal bi-isotropic media. *J. Electro. Waves Applic.*, **6**(11), 1517–1535, 1992.

[13] G. Kristensson and S. Rikte. Transient wave propagation in reciprocal bi-isotropic media at oblique incidence. *J. Math. Phys.*, **34**(4), 1339–1359, 1993.

[14] I. V. Lindell, A. H. Sihvola, S. A. Tretyakov, and A. J. Viitanen. *Electromagnetic Waves in Chiral and Bi-isotropic Media*. Artech House, Boston, London, 1994.

[15] P. Pelet and N. Engheta. The Theory of Chirowaveguides. *IEEE Trans. Antennas Propagat.*, **38**(1), 90–98, 1990.

[16] J. Reinert, G. Busse, and A. F. Jacob. Waveguide Characterization of Chiral Material: Theory. *IEEE Trans. Microwave Theory Tech.*, **47**(3), 290–296, 1999.

[17] S. Rikte. Theory of inversion of dispersive bi-isotropic slab parameters using TEM-pulses. *Wave Motion*, **32**, 1–24, 2000.

[18] S. Rikte. Reconstruction of bi-isotropic material parameters using transient electromagnetic fields. *Wave Motion*, **28**(1), 41–58, July 1998.

[19] S. Rikte. The theory of the propagation of TEM-pulses in dispersive bi-isotropic slabs. *Wave Motion*, **29**(1), 1–21, January 1999.

[20] J. A. Stratton. *Electromagnetic Theory*. McGraw-Hill, New York, 1941.

[21] J. A. M. Svedin. Propagation Analysis of Chirowaveguides Using the Finite-Element Method. *IEEE Trans. Microwave Theory Tech.*, **38**(10), 1448–1496, 1990.